

SIMULATION AND MEASUREMENT OF FLOW FIELD IN MICROCHIP

CHUAN WANG*, ZHIHUA DING^{*,†}, JIE MENG* and BINGLUN YIN[†]

**State Key Lab of Modern Optical Instrumentation, Zhejiang University
38 Zheda Rd., Hangzhou 310027, P. R. China*

*†School of Aeronautics and Astronautics, Zhejiang University
38 Zheda Rd., Hangzhou 310027, P. R. China*

†zh_ding@zju.edu.cn

Cancer (malignant tumor) is one of the serious threats to human life, causing 13% of all human deaths. A crucial step in the metastasis cascade of cancer is hematogenous spreading of tumor cells from a primary tumor. Thus, isolation and identification of cells that have detached from the primary tumor and circulating in the bloodstream (circulating tumor cells, CTCs) is considered to be a potential alternation to detect, characterize, and monitor cancer. Current methods for isolating CTCs are limited to complex analytic approaches that generate very low yield and purity. Here, we propose a high throughput 3D structured microfluidic chip integrated with surface plasmon resonance (SPR) sensor to isolate and identify CTCs from peripheral whole blood sample. The microfluidic velocity-field within the channel of the chip is mediated by an array of microposts protruding from upper surface of the channel. The height of microposts is shorter than that of the channel, forming a gap between the microposts and the lower surface of the channel. The lower surface of the channel also acts as the SPR sensor which can be used to identify isolated CTCs. Microfluidic velocity-field under different parameters of the arrayed microposts is studied through numerical simulation based on finite element method. Measurement on one of such fabricated microchips is conducted by our established optical Doppler tomography technique benefiting from its noninvasive, noncontact, and high-resolution spatial-resolved capabilities. Both simulation and measurement of the microfluidic velocity-field within the structured channel demonstrates that it is feasible to introduce fluidic mixing and causes perpendicular flow component to the lower surface of the channel by the 3D structured microposts. Such mixing and approaching capabilities are especially desirable for isolation and identification of CTCs at the coated SPR sensor.

Keywords: Circulating tumor cells (CTCs); optical Doppler tomography (ODT); microfluidic chip.

1. Introduction

Cancer is the second most common cause of death in the world, exceeded only by death from heart disease. 7.6 million people died from cancer in the world during 2007 according to the investigation

of American Cancer Society.^{1–3} As a matter of fact, the main threat and pathologic process of cancer is the spreading of circulating tumor cells (CTCs) to other locations in the body via lymph or blood (metastasis), the intrusion on and destruction

[†]Corresponding author.

of adjacent tissues (invasion). Thus, isolation and identification of these CTCs is considered to be a potential important method to detect, characterize, and monitor cancer.

For isolation of CTCs, there is a tremendous technical challenge besides theoretically feasibility,^{3–7} because it is rarely contained in the whole blood sample, comprising as few as only one cell per 10^9 hematologic cells in the blood of patients with metastatic cancer.⁸ Among a few methods that have been developed to isolate CTCs,^{5–7} the microchip devices give us a choice for CTC isolation and identification against the challenge. They have been successfully used for many applications but also have a limited capability of very low yield to deal with the blood sample of large volumes (milliliters) of whole blood samples.⁸ For identification of CTCs, the complex biology and cytology approaches^{4–7} normally time consuming. However, the epithelial cell adhesion molecule (EP-CAM) coated surface plasmon resonance (SPR) sensor is considered to be a fast identification method.^{9–12} Here, we propose a high throughput 3D structured microfluidic channel that is able to work with SPR sensor, isolate and identify CTCs from milliliters of peripheral whole blood sample in a relatively short period of time.

In order to evaluate the characteristic of mixing and approaching of the structure mediated microchip, simulation and measurement of microfluidic velocity-field in the channel has been established. The simulation is based on finite element method by COMSOL Multiphysics software. Measurement of actual microfluidic field in the microchip requests practical measurement method with high spatial resolution, which fits the exceptional advantage of optical Doppler tomography (ODT). Given the noninvasive, noncontact nature, and high spatial resolution ($2\text{--}10\ \mu\text{m}$), ODT has a number of potentially important clinical applications including application on measurement of microfluidic velocity-field. ODT is one of the functional extension of optical coherence tomography (OCT).¹³ Doppler Effect that light interacts with moving particles, such as red blood cells (RBCs) inside biological tissues, causes Doppler frequency shift in the measured interference signal. The Doppler frequency shift is detected by heterodyne detection and translated to velocity profile. Hence, ODT is used in our previous studies.^{14,15}

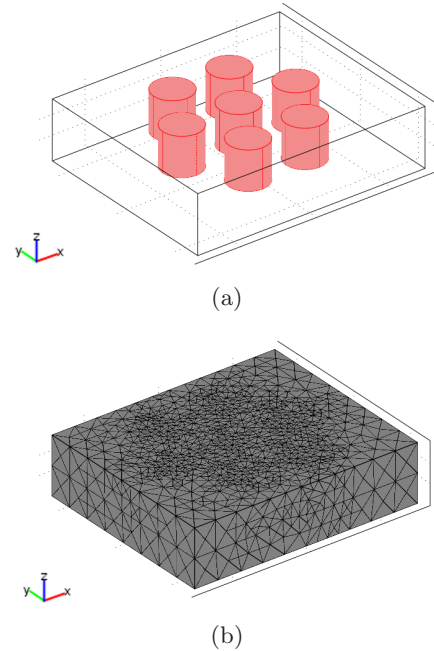


Fig. 1. Solid (a) and meshed (b) modeling of the structured channel by finite element method.

2. Method

The simulation of microfluidic velocity-field in the structured channel is established by finite element method. By COMSOL Multiphysics software, the structured channel shown in Fig. 1(a) is meshed to 12,000–26,000 spatial elements automatically depicted in Fig. 1(b). By incompressible Navier–Stokes formula, the numerical solution of each element is obtained, including viscous force in boundary elements as well as 3D velocity component and pressure. Key parameters that are used to evaluate the microchip includes velocity component in vertical and horizontal direction near the lower surface, viscous force at the lower surface, and cross-sectional velocity distribution.

The ODT system for the measurement of microfluidic field is shown in Fig. 2. The velocity is measured based on phase-resolved ODT by comparing the phase change of each pixel between sequential axial scans.^{15,16} The spatial resolution of our ODT system is $7.5\ \mu\text{m}$ and the velocity sensitivity is $10\ \mu\text{m/s}$ ($1 \times 10^{-5}\ \text{m/s}$) with a velocity range of $-6.0 \times 10^{-3}\ \text{m/s}$ to $6.0 \times 10^{-3}\ \text{m/s}$.^{14,15,17}

3. Simulation and Measurement

3.1. Simulation

Four different models with different parameters of the microposts array of the structured channel have

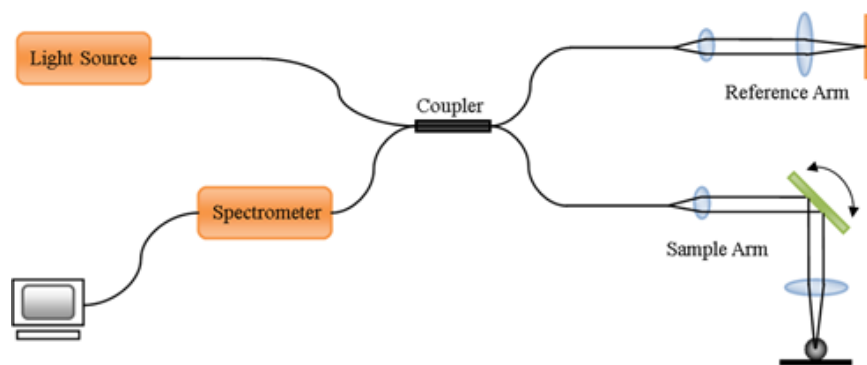


Fig. 2. Schematic of fiber-based optical Doppler tomography (ODT) system.

Table 1. Parameters of microposts array of the structured channel in simulation.

| Model | Distance (μm) | Diameter (μm) | Distribution |
|-------|----------------------------|----------------------------|------------------------------|
| 1 | 100 | 50 | Equilateral triangular array |
| 2 | 200 | 50 | Equilateral triangular array |
| 3 | 100 | 30 | Equilateral triangular array |
| 4 | 100 | 50 | Squared array |

been established in the simulation. The simulation results include velocity component in vertical direction and horizontal direction near the lower surface, viscous force at the lower surface, and cross-sectional velocity distribution. The parameters of the microposts array are shown in Table 1.

Velocity component in vertical direction near the lower surface is shown in Fig. 3. The result

indicates existence of microfluidic flow in vertical direction, and hence a mixing effect is realized.

In order to isolate the CTCs, a period of duration time of contact between CTCs and coated SPR sensor surface is required. The duration is dependent on the horizontal velocity near the lower surface. Macroscopically, the x component of this velocity is related to flux of the entire microchip and influences the isolation efficiency of the chip. Figures 4(a)–4(d) are the simulation results of horizontal velocity near lower surface based on models 1 to 4.

Simulation result of viscous force at the lower surface is shown in Fig. 5. The color bar denotes the magnitude of the viscous force at x direction. It is obvious that the structured channel with microposts array mediates the viscous force at the lower surface.

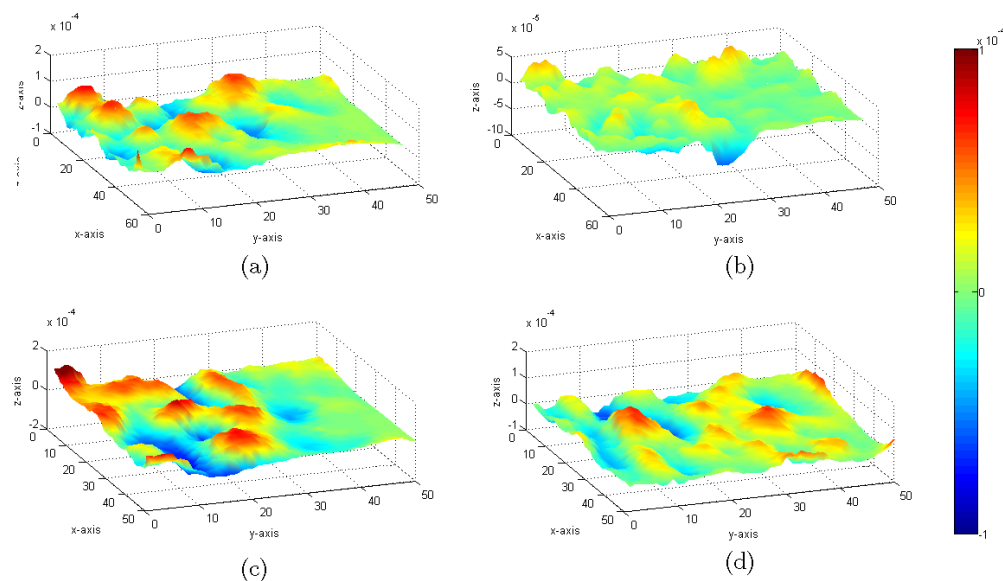


Fig. 3. Distribution of vertical velocity near the lower surface corresponding to models 1 to 4.

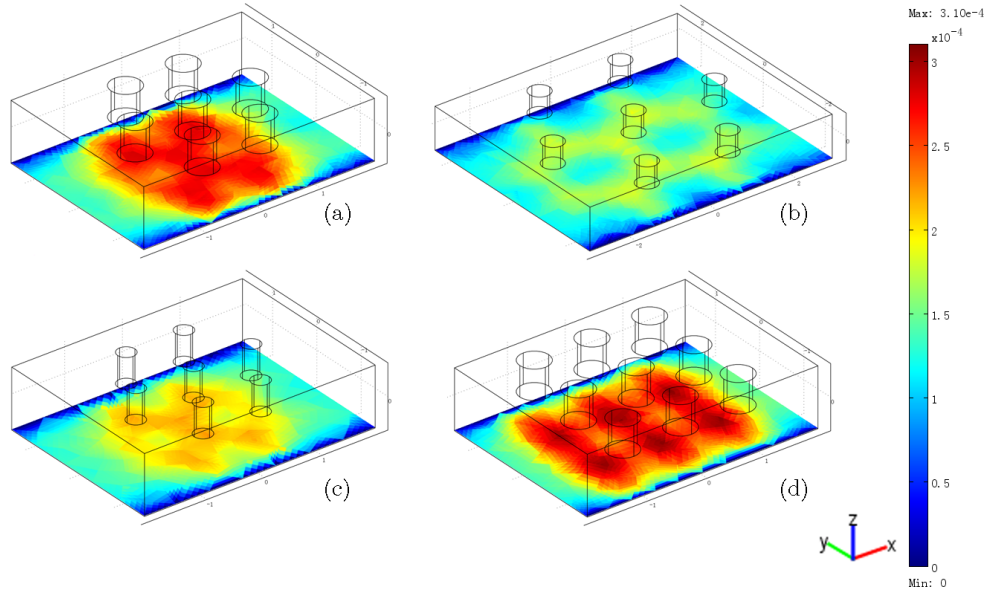


Fig. 4. Velocity component in horizontal direction near lower surface.

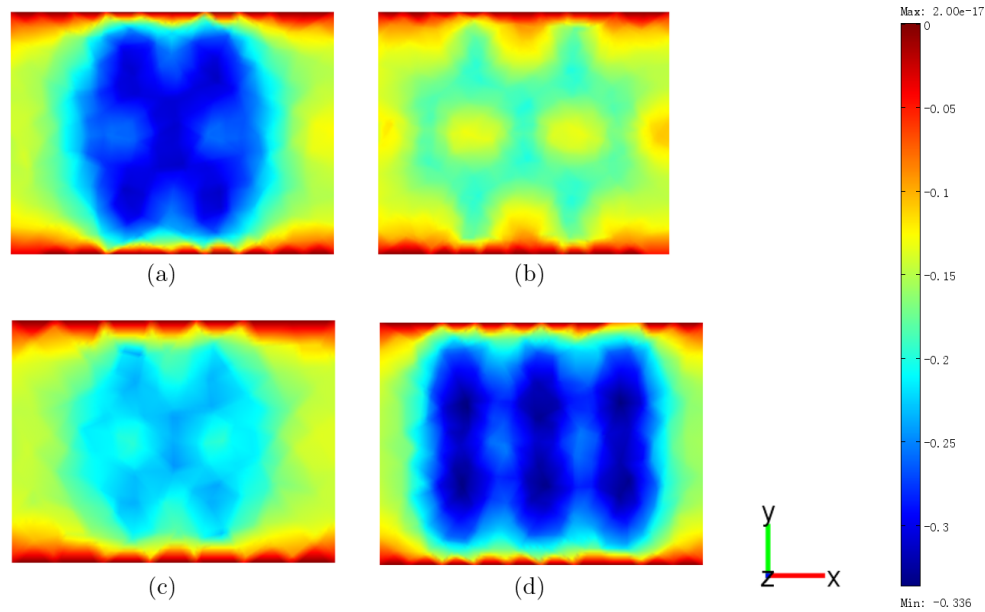


Fig. 5. Viscous force at the lower surface.

For comparison consideration, cross-sectional distribution of velocity is also simulated as shown in Fig. 6.

3.2. Measurement

Microchips having structured channel are fabricated using polydimethylsiloxane (PDMS) and one of them is measured by our ODT system. The chip under measurement is shown in Fig. 7. Parameters of microposts array in this chip is the same as that in Model 1. The diameter of micropost is

$50\ \mu\text{m}$, the distance between microposts is $100\ \mu\text{m}$, and equilateral triangle distribution of the microposts is arranged.

Aqueous solution of polystyrene beads is adopted instead of actual blood sample, the concentration is 25% and diameter of the polystyrene beads is $0.53\ \mu\text{m}$. Cross-sectional images of the microfluidic chip are shown in Fig. 8.

Figure 8(a) is the structural image of the microchip, and the brighter area denoting the flowing solution. The measured velocity distribution is shown in Fig. 8(b), corresponding to the simulation

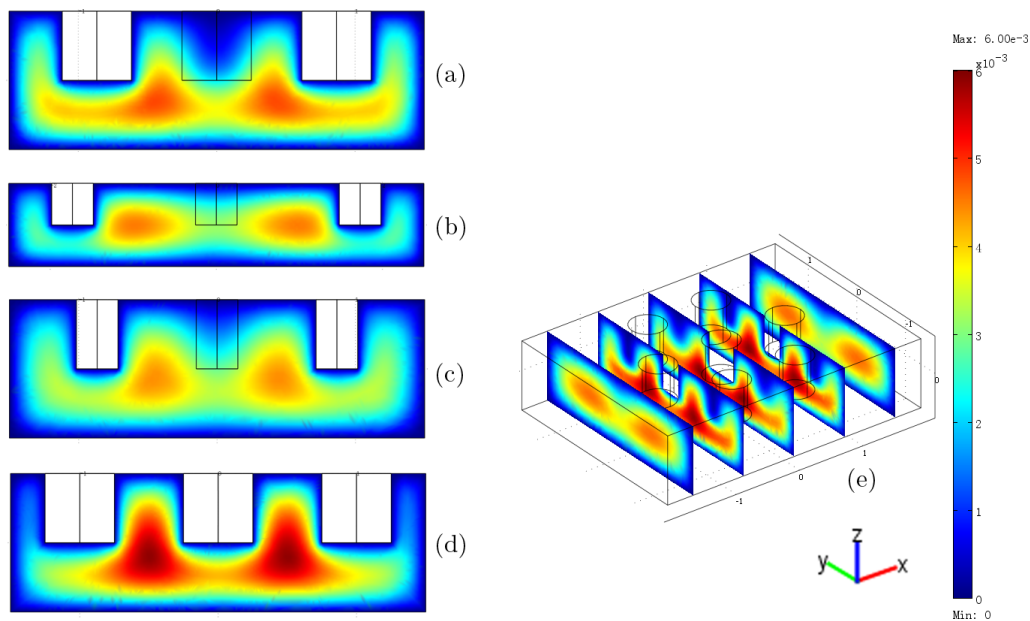


Fig. 6. Cross-sectional distribution of velocity.

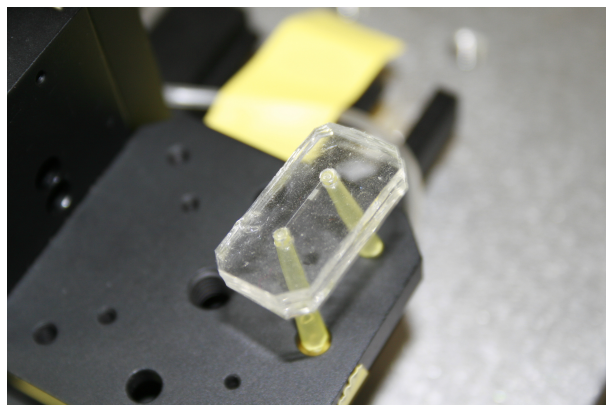


Fig. 7. Microchip used in measurement.

velocity distribution of Fig. 8(c). The magnitude of the velocity is represented by the color bar at right side of Fig. 8. Red area in Figs. 8(b) and 8(c) is the position with higher velocity. The velocity distributions of simulated and measured are not exactly the same, because of fabrication precision in microchip and difference between aqueous solution of polystyrene beads used in measurement and ideal water used in simulation.

4. Conclusion

A high throughput 3D structured microfluidic channel that is able to be integrated with SPR sensor

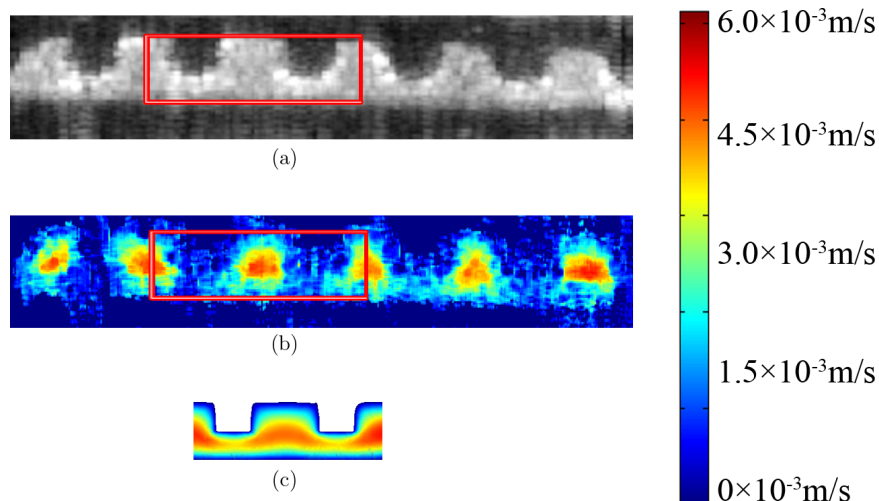


Fig. 8. Measurement and simulation results of cross-sectional distribution of velocity.

to isolate and identify CTCs from peripheral whole blood sample is proposed. Previous works on the simulation and measurement of microfluidic field in this structured channel with microposts array is presented. The microfluidic field in the channel is mediated by column microposts protruding from upper surface of the channel. A gap between the microposts and the lower surface of the channel is formed because the different height of the channel and the microposts array. Microfluidic field under different distributions, diameters of the microposts, and distances between them are simulated using finite element method by COMSOL Multiphysics software and measurement on sample microchip is conducted using ODT method through calculating the Doppler frequency shift based on phase-resolved. Simulation of microfluidic field within the structured channel demonstrates that it is feasible to introduce fluidic mixing and causes perpendicular flow component to the lower surface of the channel by the 3D structured microposts with appropriate parameters. And measurement confirms the simulation result by obtaining approximate cross-sectional distribution of velocity. Such mixing and approaching characteristics are especially desirable for capture and identify CTCs at the SPR sensor plane.

Acknowledgments

This work was supported by National High Technology Research and Development Program of China (2006AA02Z4E0) and Natural Science Foundation of China (60878057, 60978037).

References

1. A. Jemal, R. Siegel, E. Ward, Y. Hao, J. Xu, T. Murray, M. J. Thun, "Cancer statistics, 2008," *CA Cancer J. Clin.* **58**, 71–96 (2008).
2. R. A. Smith, V. Cokkinides, H. J. Eyre, "American cancer society guidelines for the early detection of cancer, 2006," *CA Cancer J. Clin.* **56**, 11–25 (2006).
3. A. Rolle, U. Pachmann, B. Willen, K. Pachmann, "Increase in number of circulating disseminated epithelial cells after surgery for non-small cell lung cancer monitored by MAINTRAC is a predictor for relapse: A preliminary report," *World J. Surg. Oncol.* **3**, 18 (2005).
4. V. Zieglschmid, C. Hollmann, O. Bocher, "Detection of disseminated tumor cells in peripheral blood," *Crit. Rev. Clin. Lab. Sci.* **42**, 155–196 (2005).
5. H. J. Kahn, A. Presta, L. Y. Yang, J. Blondal, M. Trudeau, L. Lickley, C. Holloway, D. R. McCready, D. Maclean, A. Marks, "Enumeration of circulating tumor cells in the blood of breast cancer patients after filtration enrichment: Correlation with disease stage," *Breast Cancer Res. Treat.* **86**, 237–247 (2004).
6. R. T. Krivacic, A. Ladanyi, D. N. Curry, H. B. Hsieh, P. Kuhn, D. E. Bergsrud, J. F. Kepros, T. Barbera, M. Y. Ho, L. B. Chen, "A rare-cell detector for cancer," *Proc. Nat. Acad. Sci. U. S. A.* **101**, 10501–10504 (2004).
7. E. Racila, D. Euhus, A. J. Weiss, C. Rao, J. McConnell, L. Terstappen, J. W. Uhr, "Detection and characterization of carcinoma cells in the blood," *Proc. Natl. Acad. Sci. U. S. A.* **95**, 4589–4594 (1998).
8. S. Nagrath, L. V. Sequist, S. Maheswaran, D. W. Bell, D. Irimia, L. Ulkus *et al.*, "Isolation of rare circulating tumour cells in cancer patients by microchip technology," *Nature* **450**, 1235–1239 (2007).
9. L. Huang, S. J. Maerkl, O. J. Martin, "Integration of plasmonic trapping in a microfluidic environment," *Opt. Express* **17**, 6018–6024 (2009).
10. L. Huang, W. Zhang, S. Maerkl, O. J. Martin, "Plasmonic trapping for nanoscale analysis in lab-on-the-chip applications," *Frontiers in Optics*, Paper FME3 (2008).
11. K. Narasimhan, Z. Changqing, M. Choolani, "Ovarian cancer proteomics: Many technologies one goal," *Prot. Clin. Appl.* **2**, 195–218 (2008).
12. O. H. J. Szolar, S. Stranner, I. Zinoecker, G. C. Mudde, G. Himmler, G. Waxenecker, A. Nechansky, "Qualification and application of a surface plasmon resonance-based assay for monitoring potential HAAA responses induced after passive administration of a humanized anti Lewis-Y antibody," *J. Pharm. Biomed. Anal.* **41**, 1347–1353 (2006).
13. D. Huang, E. A. Swanson, C. P. Lin, J. S. Schuman, W. G. Stinson, W. Chang, M. R. Hee, T. Flotte, K. Gregory, C. A. Puliafito, "Optical coherence tomography," *Science* **254**, 1178–1181 (1991).
14. Z. Ding, Y. Zhao, H. Ren, J. Nelson, Z. Chen, "Real-time phase-resolved optical coherence tomography and optical Doppler tomography," *Opt. Express* **10**, 236–245 (2002).
15. J. Meng, Z. Ding, Y. Yang, Z. Guo, "Study on cerebral microcirculation by Optical Doppler Tomography," *Sci. Chin. Ser. G Phys. Mech. Astron.* **51**, 1883–1891 (2008).
16. A. F. Fercher, W. Drexler, C. K. Hitzenberger, T. Lasser, "Optical coherence tomography-principles and applications," *Rep. Prog. Phys.* **66**, 239–303 (2003).
17. K. Wang, Z. Ding, T. Wu, C. Wang, J. Meng, M. Chen, L. Xu, "Development of a non-uniform discrete Fourier transform based high speed spectral domain optical coherence tomography system," *Opt. Express* **17**, 12121–12131 (2009).